

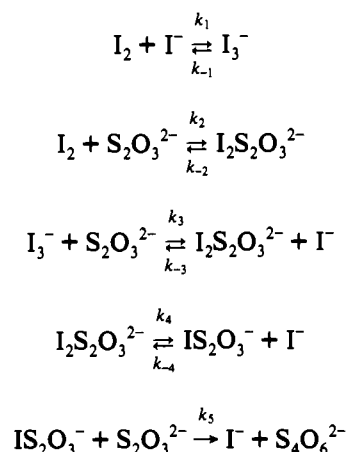
Non-Metal Redox Kinetics: Reactions of Iodine and Triiodide with Thiosulfate via $I_2S_2O_3^{2-}$ and $IS_2O_3^-$ Intermediates

William M. Scheper and Dale W. Margerum*

Department of Chemistry, Purdue University, West Lafayette, Indiana 47907

Received June 4, 1992

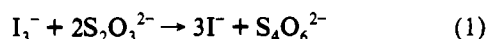
Aqueous iodine and triiodide ion react rapidly with thiosulfate ion in a multistep mechanism:



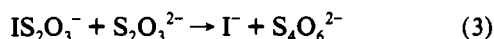
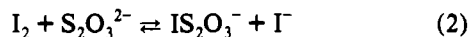
Rate constants (25.0 ± 0.2 °C, $\mu = 0.10$ M) measured by pulsed-accelerated-flow and stopped-flow methods are as follows: $k_2 = 7.8 \times 10^9$ M⁻¹ s⁻¹, $k_{-2} = 2.5 \times 10^2$ s⁻¹, $k_3 = 4.2 \times 10^8$ M⁻¹ s⁻¹, $k_{-3} = 9.5 \times 10^3$ M⁻¹ s⁻¹, $k_4/k_{-4} = 0.245$ M, $k_5 = 1.29 \times 10^6$ M⁻¹ s⁻¹. The $I_2S_2O_3^{2-}$ adduct is thermodynamically stable ($k_2/k_{-2} = K_2 = 3.2 \times 10^7$ M⁻¹), but is kinetically reactive. It dissociates rapidly to give $IS_2O_3^-$ which reacts with $S_2O_3^{2-}$ to eliminate I⁻ and form $S_4O_6^{2-}$.

Introduction

The reaction between triiodide ion and thiosulfate ion to give iodide ion and tetrathionate ion (eq 1) is one of the more widely

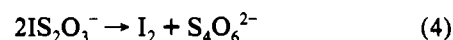


used titrimetric methods for chemical analysis.¹⁻³ The reaction is very rapid and the stoichiometry is well established. The kinetics and mechanism of the reaction have been of interest for many years. In the early 1900's, Raschig^{4,5} discovered that small amounts of $S_2O_3^{2-}$ induced the reaction between I_2 and N_3^- to give I⁻ and N₂. He proposed that the reaction between iodine and thiosulfate occurs in steps with $IS_2O_3^-$ as an intermediate (eqs 2 and 3). When the $S_2O_3^{2-}/I_2$ ratio is 2 or greater, the



reactions are extremely fast. In 1940, Chance⁶ attempted unsuccessfully to measure the rate of loss of I_2 in a rapid mixing device; he reported that the rate constant for eq 2 was greater than 3×10^7 M⁻¹ s⁻¹.

In 1949, Dodd and Griffith⁷ showed that mixtures of $S_2O_3^{2-}$ and excess I_2 form an intermediate that generates $S_4O_6^{2-}$ at a measurable rate. They followed the reaction by titration of aliquots that were withdrawn and added to a standard "indicator" solution of I_2 , KI, NaN₃, and acetate buffer. The overall process postulated was given by eq 4, and the proposed mechanism was



based on the forward reaction in eq 3 followed by the rapid reverse reaction in eq 2. They attempted to evaluate the equilibrium constant in eq 5 by a trial and error procedure to obtain the best

$$K = \frac{[S_2O_3^-][I^-]}{[S_2O_3^{2-}][I_2]} \quad (5)$$

fit of their data. They estimated that $K = 330$ at 20 °C, $\mu = 0.10$ M. We show that this estimate is 4 orders of magnitude too small. As a result, their estimated rate constant of 140 M⁻¹ s⁻¹ for the reaction of $IS_2O_3^-$ with $S_2O_3^{2-}$ (eq 3) is also 4 orders of magnitude too small.

In 1951, Awtrey and Connick⁸ followed the reaction in eq 4 spectrophotometrically by observing the formation of I_3^- , which is in rapid equilibrium with I_2 (eq 6). They used a "small mixing

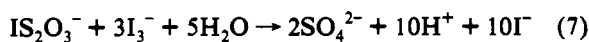


device" attached to a spectrophotometer and measured the absorbance increase of I_3^- over a period of 10-400 s. An integrated rate expression fits the data and they reported observed rate

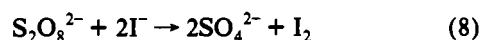
- (1) Kolthoff, I. M.; Sandell, E. B.; Meehan, E. J.; Bruckenstein, S. *Quantitative Chemical Analysis*, 4th ed.; Macmillan: London, 1969; pp 842-864.
- (2) Laitinen, H. A.; Harris, W. E. *Chemical Analysis*, 2nd ed.; McGraw-Hill: New York, 1975; pp 351-357.
- (3) Harris, Daniel C. *Quantitative Chemical Analysis*, 3rd ed.; Freeman: New York, 1991; pp 403-406.
- (4) Raschig, F. *Chem. Ztg.* **1908**, *32*, 1203.
- (5) Raschig, F. *Ber. Dtsch. Chem. Ges.* **1915**, *48*, 2088.
- (6) Chance, B. *J. Franklin Inst.* **1940**, *229*, 756.

- (7) Dodd, G.; Griffith, R. O. *Trans. Faraday Soc.* **1949**, *45*, 546-563.
- (8) Awtrey, A. D.; Connick, R. E. *J. Am. Chem. Soc.* **1951**, *73*, 1341-1348.

constants with an accuracy of $\pm 10\%$. The observed combination of constants ($119 \text{ M}^{-2} \text{ s}^{-1}$) was the ratio of the rate constant for eq 3 and equilibrium constants for eqs 2 and 6. Our results are in excellent agreement with this ratio at lower concentrations of iodide ion. Awtrey and Connick attempted to measure the rate constant for reaction 2 by use of a "fast mixing device", which was a crude continuous flow apparatus with a mixing time of about 0.13 s. The reaction was too fast to measure and they reported that the rate constant must be greater than $8 \times 10^6 \text{ M}^{-1} \text{ s}^{-1}$. At low iodide ion concentrations (less than $3 \times 10^{-3} \text{ M}$ $[\text{I}^-]$), they found that other reactions occurred that gave sulfate ion as a product (the stoichiometry is given in eq 7), as well as the tetrathionate ion product from eq 3.



Rao and Mali⁹ used electrochemical detection of I_2 under conditions where it was slowly generated from the reaction of peroxodisulfate ion and iodide ion (eq 8) with the rate expression in eq 9. Since I_2 was generated in the presence of $\text{S}_2\text{O}_3^{2-}$, the



$$\frac{d[\text{I}_2]}{dt} = 3 \times 10^{-3} [\text{S}_2\text{O}_8^{2-}] [\text{I}^-] \quad (9)$$

concentration of I_2 was extremely low because of its fast reaction with $\text{S}_2\text{O}_3^{2-}$. They reported I_2 levels in the 10^{-8} M range and from these values gave a rate constant of $1.5 \times 10^5 \text{ M}^{-1} \text{ s}^{-1}$ for the reaction of I_2 and $\text{S}_2\text{O}_3^{2-}$ in the presence of 0.01 M I^- . Our work shows that this rate constant is a factor of 7700 too small. Their $\text{I}_2 + \text{I}_3^-$ concentration levels should have been in the 10^{-13} M range, which is many orders of magnitude below the lowest concentration (10^{-6} M) used for their calibration curve. Alternatively, it may be that the $\text{S}_2\text{O}_8^{2-}$ and I^- reaction is catalyzed by the presence of $\text{S}_2\text{O}_3^{2-}$ or IS_2O_3^- . Their paper⁹ is novel in its measurement of a rate constant from the concentration of a steady-state species (I_2), but it is erroneous in its calculations and in its final interpretation.

The pulsed-accelerated-flow (PAF) method¹⁰⁻¹² and the intense absorbance of I_3^- make it possible in the present work to use pseudo-first-order conditions with excess $\text{S}_2\text{O}_3^{2-}$ and excess I^- and still measure second-order rate constants that are as large as the diffusion limit ($\sim 7 \times 10^9 \text{ M}^{-1} \text{ s}^{-1}$ at 25°C in water) for the reaction of I_2 with $\text{S}_2\text{O}_3^{2-}$. Stopped-flow methods with excess I_2 or with excess $\text{S}_2\text{O}_3^{2-}$ permit direct evaluation of rate constants for the slower reaction (eq 3). Thus, 84 years after Raschig's proposed reactions (eqs 2 and 3) we are finally able to measure the rate and equilibrium constants for this system. At high iodide ion concentrations, we have evidence for the presence of $\text{I}_2\text{S}_2\text{O}_3^{2-}$ as well as IS_2O_3^- .

Experimental Section

Reagents. Analytical reagent grade NaIO_3 was recrystallized from water and dried at 130°C for 12 h. Triiodide solutions were made by the reaction of NaIO_3 with I^- and H^+ and adjusted to a final pH of 3–4. Sodium thiosulfate solutions were prepared in freshly boiled, distilled, deionized water and stored at pH 9–10, to prevent bacterial degradation. The $\text{S}_2\text{O}_3^{2-}$ solutions were standardized iodometrically with primary standard grade KIO_3 . Sodium iodide solutions were flushed with argon to remove dissolved oxygen. The NaI stock solution was stored in the dark and standardized by addition of Br_2 to oxidize I^- to IO_3^- and then

titrated iodometrically with $\text{S}_2\text{O}_3^{2-}$. Ionic strength was controlled with NaClO_4 , which was recrystallized from water.

Methods. UV-vis spectra were recorded on a Perkin-Elmer 320 spectrophotometer. Solution pH values were measured with a Sargent-Welch Model S-30072-15 combination electrode and an Orion Model 701A pH meter. Hydrogen ion concentrations were calculated from the pH measurements ($\text{p}[\text{H}^+] = 0.9820 \times \text{pH} + 0.25$) at $\mu = 0.10 \text{ M}$ (NaClO_4) based on the electrode response to titrations of NaOH with HClO_4 . All reactions were run between $\text{p}[\text{H}^+]$ 3 and 4.

A Dionex-Durrum Model D-110 stopped-flow spectrophotometer (1.88 cm cell path) interfaced to a Zenith 151 PC with a MetraByte DASH-16 A/D converter was used to collect kinetic data. These experiments were monitored at 353 nm for the appearance or disappearance of I_3^- ($\epsilon = 26,400 \text{ M}^{-1} \text{ cm}^{-1}$).⁸ The $\text{I}_2\text{S}_2\text{O}_3^{2-}$ and IS_2O_3^- intermediates do not have appreciable absorbances at this wavelength. All reactions were run at $25.0 \pm 0.2^\circ \text{C}$ and $\mu = 0.10 \text{ M}$ (NaClO_4).

First-order rate constants were evaluated from plots of $\ln(A - A_\infty)$ against time. In order to extend the accessibility of first-order rate constants from stopped-flow experiments and to achieve more accurate rate constants, all k_{obsd} values greater than 100 s^{-1} were corrected for the mixing rate constant (eq 10).¹³ For this instrument, k_{mix} has been

$$k_r = \frac{k_{\text{obsd}}}{1 - \frac{k_{\text{obsd}}}{k_{\text{mix}}}} \quad (10)$$

determined to be 1700 s^{-1} . By this correction, systematic errors due to the limitations of mixing rates are accounted for, and first-order rate constants (k_{obsd}) above 100 s^{-1} can be accurately determined.

Pulsed-Accelerated-Flow Method. A pulsed-accelerated-flow spectrophotometer, model IV, was used to obtain kinetic data for the reactions of iodine and triiodide with thiosulfate. This instrument has a wavelength range of 200–850 nm, and improvements in the optics led to much higher light throughput as compared with earlier models.¹¹ The PAF employs integrating observation during continuous flow mixing of short duration (a 0.4-s pulse). The purpose of the pulsed flow is to conserve reagents. The reactants are observed along the direction of flow from their point of mixing to their exit from the observation tube (1.025 cm). A twin-path mixing/observation cell made from PVC is used. In this study, the flow was decelerated during the pulse to give a linear velocity ramp, and 250 measurements of the transmittance were taken as the flow velocity in the observation tube changed from 12.5 to 3.0 m s^{-1} . The velocity variation permits the chemical-reaction-rate process to be resolved from the mixing-rate process. The method of observation, the efficient mixing, and the variation of flow velocity permit accurate measurement of first-order rate constants that are factors of 10^3 larger than can be measured by typical stopped-flow methods. Solution reservoirs, drive syringes, and the mixing/observation cell were thermostated at $25.0 \pm 0.2^\circ \text{C}$ with a circulating water bath. Reactant solutions were drawn directly from the reservoirs into the drive syringes through Teflon tubing. Equation 11 is

$$M_{\text{exp}} = \frac{A_v - A_\infty}{A_0 - A_\infty} = \frac{1}{bk_m} + \frac{v}{bk_r} \quad (11)$$

used in the analysis of PAF data under pseudo-first-order conditions (when $k_r < 60,000 \text{ s}^{-1}$), where M_{exp} is the defined absorbance ratio, A_v is the absorbance of the reaction mixture at a given instantaneous velocity, A_∞ is the absorbance at infinite time for the reaction under investigation, A_0 is the absorbance at time zero, k_r is the reaction rate constant (s^{-1}), b is the reaction path length (0.01025 m), v is the solution velocity in the observation tube (m s^{-1}), and k_m is a proportionality constant from the mixing rate constant (k_{mix}) where $k_m = k_{\text{mix}}/v$. Linear plots of M_{exp} vs v have slopes of $1/(bk_r)$, for first-order reactions. For rate constants greater than $60,000 \text{ s}^{-1}$, the kinetic data are analyzed by eq 12. The c/v term is necessary when the extent of reaction in the center of the mixing cell becomes appreciable.^{14,15}

All kinetic data obtained on the PAF spectrophotometer were collected at $\mu = 0.10 \text{ M}$ (NaClO_4) and 25°C by following the disappearance of

(9) Rao, T. S.; Mali, S. I. Z. *Naturforsch.* 1974, 29a, 141–144.

(10) Jacobs, S. A.; Nemeth, M. T.; Kramer, G. W.; Ridley, T. Y.; Margerum, D. W. *Anal. Chem.* 1984, 56, 1058–1065.

(11) Nemeth, M. T.; Fogelman, K. D.; Ridley, T. Y.; Margerum, D. W. *Anal. Chem.* 1987, 59, 283–291.

(12) Fogelman, K. D.; Walker, D. M.; Margerum, D. W. *Inorg. Chem.* 1989, 28, 986–993.

(13) Dickson, P. N.; Margerum, D. W. *Anal. Chem.* 1986, 58, 3153–3158.

(14) Troy, R. C.; Kelley, M. D.; Nagy, J. C.; Margerum, D. W. *Inorg. Chem.* 1991, 30, 4838–4845.

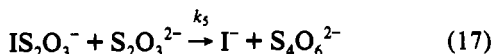
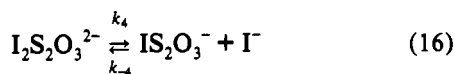
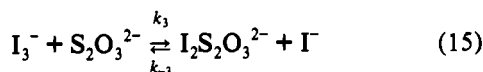
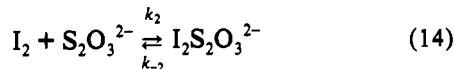
(15) Bowers, C. P.; Fogelman, K. D.; Nagy, J. C.; Ridley, T. Y.; Wang, Y. L.; Evetts, S. W.; Margerum, D. W. To be submitted for publication.

$$M_{\text{exp}} = \frac{1}{bk_m} + \frac{v}{bk_r} + \frac{c}{v} \quad (12)$$

I_3^- at 353 nm. The k_i values reported in the tables are averages of four to five trials. The values in parentheses denote 1 standard deviation in the last digit.

Results and Discussion

Proposed Mechanism. We propose the reaction mechanism given in eqs 13–17. The rate constants for eq 13 (25 °C) are



known from two independent temperature-jump relaxation studies.^{16,17} The study¹⁶ in a 50% D₂O–H₂O mixture at $\mu = 0.02$ M gave $k_1 = (6.2 \pm 0.8) \times 10^9$ M⁻¹ s⁻¹ and $k_{-1} = (8.5 \pm 1.0) \times 10^6$ s⁻¹. The study¹⁷ in 100% H₂O at $\mu = 0.001$ – 0.006 M gave $k_1 = (5.6 \pm 0.6) \times 10^9$ M⁻¹ s⁻¹ and $k_{-1} = (7.5 \pm 0.8) \times 10^6$ s⁻¹. Equilibrium measurements¹⁸ give a K_1 value of 721 M⁻¹ at 25.0 ± 0.2 °C that has been shown to be relatively independent of ionic strength. The mechanism in eqs 14–17 is similar to that proposed by Raschig⁵ and others^{7,8} except $I_2S_2O_3^{2-}$ is added as an intermediate, because our results require this species at higher I^- concentrations (above 0.02 M).

Stopped-Flow Methods. Stopped-flow kinetics were performed under two sets of conditions. In the first series of experiments, both the $[I^-]$ and the $[S_2O_3^{2-}]$ were in large excess over the initial $[I_2]_T$, where $[I_2]_T = [I_2] + [I_3^-]$. The second series of experiments had only $[I^-]$ in large excess, and the initial $[I_2]_T$ was in stoichiometric excess over the initial $[S_2O_3^{2-}]$. In both sets of experiments the reactions of I_2 and I_3^- with $S_2O_3^{2-}$ are assumed to be very fast and are treated as preequilibria. This assumption is verified in the PAF study. The rate-determining step is the reaction of $IS_2O_3^-$ with $S_2O_3^{2-}$, and the I_3^- absorbance is used as an indicator for the reaction.

Stopped-Flow Experiments with Excess $[S_2O_3^{2-}]$ and $[I^-]$. The reaction between I_3^- and $S_2O_3^{2-}$ was studied as a function of $[S_2O_3^{2-}]$ with a stopped-flow spectrophotometer in order to determine the rate of the reaction between $IS_2O_3^-$ with $S_2O_3^{2-}$. If we assume that the mechanism involves the initial formation of $I_2S_2O_3^{2-}$ followed by an equilibrium between $I_2S_2O_3^{2-}$ and $IS_2O_3^-$, with the $IS_2O_3^-$ as the reactive species, the rate law is shown in eqs 18–21. Under our experimental conditions, the values for the concentrations of $[I_2]$ (eq 19) and $[I^-]^2$ (eq 21) are both negligible relative to other terms in these equations. The corrected first-order rate constants (Table I) can be simplified to eq 22, where $[I^-]$ is constant at 50 mM. This plot is shown

Table I. Stopped-Flow Data for the Reaction of I_2/I_3^- with Excess $S_2O_3^{2-}$

$10^5[I_2]_T$, M	$10^4[S_2O_3^{2-}]$, M	k_r , ^a s ⁻¹
1.03	0.98	87 (9)
1.03	1.23	109 (8)
1.03	1.47	140 (10)
1.03	1.96	210 (20)
1.07	2.03	250 (20)
1.56	2.94	310 (30)
1.56	3.04	330 (50)

^a Conditions: $\mu = 0.10$ M (NaClO₄); 25.0 ± 0.2 °C; 353 nm; 1.88-cm light path; $[I^-] = 0.050$ M.

in Figure 1; the slope is $1.07(4) \times 10^6$ M⁻¹ s⁻¹ and the intercept is statistically indistinguishable from zero.

$$\frac{d[S_4O_6^{2-}]}{dt} = \frac{-d[I_3^-]_T}{dt} = k_5[S_2O_3^{2-}][IS_2O_3^-] \quad (18)$$

$$[I_3^-]_T = [I_3^-] + [I_2] + [I_2S_2O_3^{2-}] + [IS_2O_3^-] \quad (19)$$

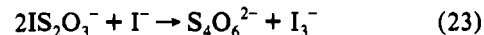
$$[IS_2O_3^-] = \frac{K_3K_4[S_2O_3^{2-}][I_3^-]_T}{K_3K_4[S_2O_3^{2-}] + K_3[S_2O_3^{2-}][I^-] + [I^-]^2} \quad (20)$$

$$\frac{-d[I_3^-]_T}{dt} = \left(\frac{k_5K_3K_4[S_2O_3^{2-}]^2}{K_3K_4[S_2O_3^{2-}] + K_3[S_2O_3^{2-}][I^-] + [I^-]^2} \right) [I_3^-]_T \quad (21)$$

$$k_r = \frac{k_5K_4[S_2O_3^{2-}]}{K_4 + [I^-]} \quad (22)$$

The I^- concentration was not varied in these experiments because high concentrations of I^- were needed to give measurable I_3^- concentrations. The initial reaction is very fast and the total I_2 concentration is small after the preequilibria between I^- , I_2 , I_3^- , $I_2S_2O_3^{2-}$, and $IS_2O_3^-$ are established.

I_3^- Re-formation Experiments. The second set of stopped-flow experiments was run with the initial $[S_2O_3^{2-}]$ less than the stoichiometric concentration of total I_2 . Our results are similar to the experimental observations reported by Awtrey and Connick.⁸ On the basis of their mechanism, which has only $IS_2O_3^-$ as an intermediate, an initial decrease in the I_3^- absorbance occurs immediately and a preequilibrium with I_3^- is established. At longer times, as $S_2O_3^{2-}$ and $IS_2O_3^-$ react to form $S_4O_6^{2-}$, the preequilibrium shifts back to reactants, and the absorbance due to I_3^- increases. The overall stoichiometry is shown in eq 23. This absorbance increase is relatively slow, because the $S_2O_3^{2-}$ concentration is very small after the fast preequilibria steps.



Awtrey and Connick gave the integrated rate expression in eqs 24–25, based on the rate expression in eq 26 and the assumption that $[IS_2O_3^-] = 2([I_2]_{T\infty} - [I_2]_T)$ for the net reaction in eq 23.

$$\frac{([I_2]_T)_\infty}{([I_2]_T)_\infty - ([I_2]_T)_t} + \ln \left(\frac{([I_2]_T)_\infty - ([I_2]_T)_t}{([I_2]_T)_\infty - ([I_2]_T)_e} \right) = k_r t + c \quad (24)$$

$$c = \frac{([I_2]_T)_\infty}{([I_2]_T)_\infty - ([I_2]_T)_e} + \ln \left(\frac{([I_2]_T)_\infty - ([I_2]_T)_e}{([I_2]_T)_\infty - ([I_2]_T)_e} \right) \quad (25)$$

$$\frac{d[S_4O_6^{2-}]}{dt} = \frac{d[I_2]_T}{dt} = k_5[S_2O_3^{2-}][IS_2O_3^-] \quad (26)$$

In eq 25 ($[I_2]_T)_e$ refers to the concentration found after the initial

(16) Turner, D. H.; Flynn, G. W.; Sutin, N.; Beitz, J. V. *J. Am. Chem. Soc.* **1972**, *94*, 1554–1559.

(17) Ruasse, M.; Aubard, J.; Galland, B.; Adenier, A. *J. Phys. Chem.* **1986**, *90*, 4382–4388.

(18) Ramette, R. W.; Sandford, R. W. *J. Am. Chem. Soc.* **1965**, *87*, 5001–5005.

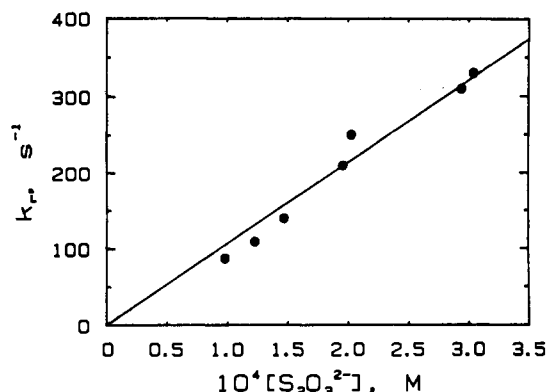


Figure 1. Dependence of the pseudo-first-order rate constant (k_r) on the $S_2O_3^{2-}$ concentration for the reaction of $IS_2O_3^-$ with $S_2O_3^{2-}$.

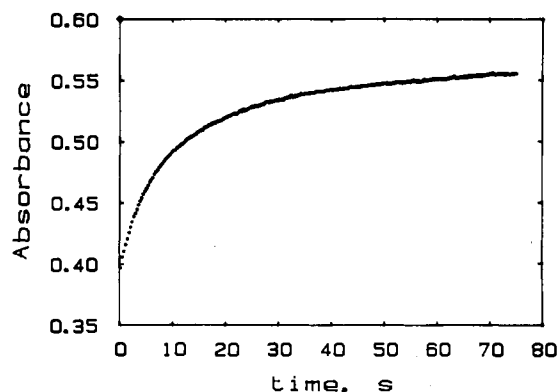


Figure 2. Experimental data for the reformation of I_3^- obtained with a stopped-flow spectrophotometer. The fit of the data to the integrated rate expression in eq 28 coincides with the experimental curve.

fast preequilibrium reaction. This leads to the expression in eq 27 for k_r , based on $K' = [IS_2O_3^-][I^-]^2 / ([I_3^-][S_2O_3^{2-}])$ and a

$$k_r = \frac{4k_5[I^-]^2(1 + K_1[I^-])}{K_1[I^-]} \quad (27)$$

negligible concentration of $I_2S_2O_3^{2-}$. Equation 24 can be expressed in terms of absorbance (eq 28), where the left-hand side vs time gives a linear plot. A weighted-least-squares regression routine

$$\frac{A_\infty}{A_\infty - A_t} + \ln(A_\infty - A_t) = k_r t + \frac{A_\infty}{A_\infty - A_c} + \ln(A_\infty - A_c) \quad (28)$$

was used for our data, where the weighting factor is given in eq 29.¹⁹ This type of weighting corrects for any bias introduced by

$$W_t = \left(\frac{1}{dY/dA_t} \right)^2 = \frac{(A_\infty - A_t)^4}{A_t^2} \quad (29)$$

the transform of the measured data to a linear function. The linear regression then minimizes the sum of the squares of the deviations in absorbance, not in the transformed Y values.

The A_∞ values used were determined by a χ^2 minimization procedure. The slope and intercept of the fit for a particular A_∞ value were used to calculate Y values, which were used to iteratively calculate absorbance values. The value of χ^2 was then calculated based on the difference between the measured and fitted absorbance values. This procedure was used to calculate χ^2 for a given value of A_∞ , and χ^2 was minimized by using Brent's algorithm.²⁰

Table II. I_3^- Re-formation Data^a

$10^5[I_2]_T$, M	$10^5[S_2O_3^{2-}]$, M	$[I^-]$, M	k_r , s ⁻¹
1.50	0.934	0.0250	0.30 ^b
1.50	0.934	0.0375	0.48 ^b
1.50	0.934	0.0500	0.77 ^b
1.50	0.934	0.0675	1.35 ^b
1.50	0.934	0.0875	2.04 ^b
1.50	0.934	0.1000	2.53 ^b
2.75	1.25	0.2000	5.8 (4) ^c
2.75	1.25	0.0500	0.75 (3)
2.75	1.25	0.0150	0.13 (3)
2.75	1.25	0.0100	0.0721 (5)
2.75	1.25	0.0050	0.032 (1)
2.70	2.75	0.0500	0.93 (4)
2.70	2.75	0.0375	0.49 (3)
2.70	2.75	0.0250	0.250 (9)
2.70	2.75	0.0125	0.087 (4)
2.70	2.75	0.0050	0.027 ^b

^a Conditions: $\mu = 0.10$ M (NaClO₄); 25.0 ± 0.2 °C; $\lambda = 353$ nm; 1.88-cm cell path. ^b Single measurement. ^c $\mu = 0.20$ M.

Figure 2 shows absorbance versus time data; the calculated curve from eq 28 coincides with these data. A series of reactions was studied where $[I^-]$ was varied from 5 to 200 mM and the ratio of $[S_2O_3^{2-}]$ to $[I_2]_T$ was varied from 1:2 to 1:1 (Table II). The lowest I^- concentration was sufficient to avoid SO_4^{2-} formation⁸ and the highest I^- concentration was a factor of 3 greater than that used by Awtrey and Connick.

A plot of $(k_r/4)(K_1[I^-]/(1 + K_1[I^-]))$ vs $[I^-]^2$ is not linear as would be required by the Awtrey and Connick⁸ mechanism (eq 27). However, below 0.02 M $[I^-]$ the plot does appear to fit this equation. At higher $[I^-]$ concentrations, the plot curves and begins to show a saturation effect.

Our proposed mechanism permits the concentration of $I_2S_2O_3^{2-}$ to be appreciable, but retains $IS_2O_3^-$ as the species that reacts with $S_2O_3^{2-}$ (eq 17). By starting with eq 18, we can derive the rate expression in eqs 30–36. This gives the same type of

$$\frac{d[I_2]_T}{dt} = \frac{k_5[IS_2O_3^-][I_2S_2O_3^{2-}][I^-]}{K_3[I_3^-]} \quad (30)$$

$$[I_2S_2O_3^{2-}]_T = [I_2S_2O_3^{2-}] + [IS_2O_3^-] \quad (31)$$

$$[I_2S_2O_3^{2-}]_T = [I_2S_2O_3^{2-}] \left(\frac{K_4 + [I^-]}{[I^-]} \right) = [IS_2O_3^-] \left(\frac{K_4 + [I^-]}{K_4} \right) \quad (32)$$

$$\frac{d[I_2]_T}{dt} = \frac{k_5 K_4 [I^-]^2 [I_2S_2O_3^{2-}]_T^2}{K_3 [I_3^-] (K_4 + [I^-])^2} \quad (33)$$

$$[I_2S_2O_3^{2-}]_T = 2([I_2]_{T\infty} - [I_2]_T) \quad (34)$$

$$[I_2]_T = [I_3^-] \left(\frac{1 + K_1[I^-]}{K_1[I^-]} \right) \quad (35)$$

$$\frac{d[I_2]_T}{dt} = \left(\frac{4k_5 K_4 [I^-]^2}{K_3 (K_4 + [I^-])^2} \right) \frac{([I_2]_{T\infty} - [I_2]_T)^2 (1 + K_1[I^-])}{[I_2]_T K_1 [I^-]} \quad (36)$$

integrated rate expression given in eq 25. However, the k_r ,

(20) Press, W. H.; Flannery, B. P.; Teukolsky, S. A.; Vetterling, W. T. *Numerical Recipes in C*, 1st ed.; Cambridge University Press: Cambridge, 1988; pp 299–302.

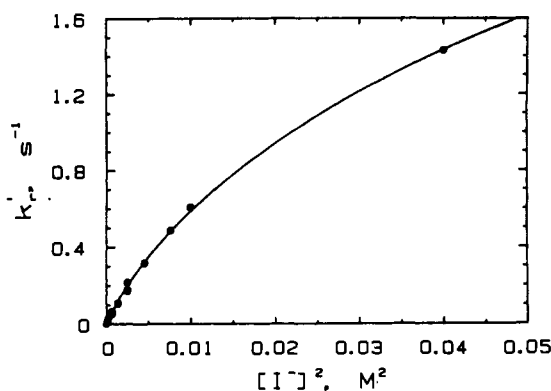


Figure 3. Dependence of the I_3^- reformation rate constant (k_r') on the concentration of $[I^-]^2$. The curve is evaluated from eq 38 where $K_4 = 0.245$ and $k_5/K_3 = 29.4$.

dependence is different as given in eq 37. Figure 3 shows a plot

$$k_r' = \frac{4k_5K_4[I^-]^2}{K_3(K_4 + [I^-])^2} \left(\frac{1 + K_1[I^-]}{K_1[I^-]} \right) \quad (37)$$

of k_r' against $[I^-]^2$, where k_r' is given by eq 38. The tendency

$$k_r' = \frac{k_r}{4} \left(\frac{K_1[I^-]}{1 + K_1[I^-]} \right) = \frac{k_5K_4[I^-]^2}{K_3(K_4 + [I^-])^2} \quad (38)$$

toward a saturation effect at high $[I^-]$ values is a result of the fact that the $[I^-]$ value becomes appreciable compared to the K_4 value. An excellent fit of the data is obtained for $K_4 = 0.245 \pm 0.009$ M and $k_5/K_3 = 29.4 \pm 0.3$ M⁻¹ s⁻¹. The k_5/K_3K_4 value of 120 ± 5 M⁻² s⁻¹ is in excellent agreement with Awtrey and Connick's value of 119 M⁻² s⁻¹. (This agreement is possible because most of their data used $[I^-]$ concentrations less than 0.03 M where $K_4/[I^-] > 8$.) When these results are combined with the stopped-flow data from eq 22 where $[S_2O_3^{2-}]$ is 10–30 times larger than $[I_2]_T$, we can calculate $k_5 = (1.29 \pm 0.04) \times 10^6$ M⁻¹ s⁻¹ and $K_3 = (4.4 \pm 0.2) \times 10^4$.

Several alternate mechanisms that were considered did not fit the data. For example, $IS_2O_3^-$ cannot be a steady-state intermediate; it must be in appreciable concentration. Also, direct attack of $S_2O_3^{2-}$ on $I_2S_2O_3^{2-}$ to give $S_4O_6^{2-}$ does not fit the data.

Stopped-Flow Studies of the I_3^- , I_2 , $I_2S_2O_3^{2-}$, $IS_2O_3^-$, and I^- Equilibria. A number of stopped-flow experiments were performed in an attempt to determine the stoichiometry of the initial reactions that occur prior to the reaction of $IS_2O_3^-$ with $S_2O_3^{2-}$, and to directly measure the equilibrium constants for these reactions. These studies were performed under similar conditions as the stopped-flow kinetic experiments ($[I^-]$ from 5 to 100 mM and the ratio $[S_2O_3^{2-}]/[I_2]_T$ varied from 1:2 to 3:2). Equilibrium absorbance data (A_e) were collected by measuring the absorbance of the reaction system between 5 and 50 ms.

Table III lists the data and values for K' (calculated from eq 39), based on the Raschig mechanism in which $IS_2O_3^-$ is the only intermediate formed. The data show more than a three-fold variation in K' , and there is a slight increase as $[I^-]$ increases.

$$K' = \frac{\left(\frac{A_i - A_e}{\epsilon b} \right) \left(1 + \frac{1}{K_1[I^-]} \right) [I^-]^2}{\left(\frac{A_e}{\epsilon b} \right) \left[[S_2O_3^{2-}]_i - \left(\frac{A_i - A_e}{\epsilon b} \right) \left(1 + \frac{1}{K_1[I^-]} \right) \right]} \quad (39)$$

Table III also lists the calculated equilibrium constant K_3 for our proposed mechanism in which $I_2S_2O_3^{2-}$ is a proposed intermediate in equilibrium with $IS_2O_3^-$. Because of the large deviations in the absorbance measurements, it was impossible to solve for K_3 and K_4 simultaneously. K_4 was therefore set equal to 0.245 M, the value determined from the kinetic data, and K_3

Table III. Stopped-Flow Determination of Equilibrium Constants^a

$[I^-]$, M	$10^5[S_2O_3^{2-}]_i$, M	A_i	A_e	$10^{-3}K'$, ^b M	$10^{-4}K_3$ ^c
0.1000	0.934	1.347	0.910	11.8	3.42
0.0875	0.934	1.059	0.651	4.92	1.48
0.0675	0.934	0.966	0.532	9.11	2.92
0.0500	0.934	0.881	0.447	7.06	2.40
0.0375	0.934	0.772	0.335	9.07	3.21
0.0250	0.934	0.799	0.370	3.52	1.31
0.0500	2.75	1.291	1.140	5.76	1.95
0.0375	2.75	1.286	0.090	7.71	2.73
0.0250	2.75	1.307	0.097	4.65	1.72
0.0125	2.75	1.258	0.052	7.97	3.10
0.0050	2.75	1.081	0.026	3.73	1.49
0.050	3.75	1.291	0.044	6.23	2.11
0.0375	3.75	1.286	0.029	5.62	1.99
0.0250	3.75	1.307	0.011	7.81	2.90
0.0125	3.75	1.258	0.005	4.60	1.79

^a Conditions: $\mu = 0.10$ M (NaClO₄); 25.0 ± 0.2 °C; $\lambda = 353$ nm; 1.88-cm path length. ^b K' assumes the $I_2S_2O_3^{2-}$ concentration to be negligible. ^c For $K_4 = 0.245$ M, average $K_3 = (2.3 \pm 0.7) \times 10^4$.

was evaluated from $K'/(K_4 + [I^-])$. The K_3 values have less variation than the K' values. The results give an average value of K_3 of $(2.3 \pm 0.7) \times 10^4$. This value is almost a factor of 2 smaller than the value determined from the kinetic data.

It should be noted that a large degree of error was expected based on the experimental conditions. The Durrum stopped-flow spectrophotometer is a single-beam instrument that is susceptible to lamp drift and electronic fluctuations. Some of the measured preequilibrium absorbances are small compared to the initial absorbance, and any small errors in the determination of A_e will have a dramatic effect on the calculated equilibrium constants. When A_e is less than 0.06, a decrease in its value of 0.01 or less will give much larger K_3 values. Finally, A_e is determined from the minimum absorbance of the dynamic system. Since we have a system where this minimum is short-lived, errors in the A_e values are unavoidable.

Qualitatively, the equilibrium data are consistent with the stopped-flow kinetic data. Both require the initial formation of an $I_2S_2O_3^{2-}$ intermediate that must be in rapid equilibrium with $IS_2O_3^-$. Because there is a larger degree of uncertainty in the pseudo equilibrium data, we believe the values determined from the resolution of the kinetic data are better estimates of the equilibrium constants for K_3 and K_4 .

Pulsed-Accelerated-Flow Reactions. Rate constants are determined for the parallel reactions of I_2 and I_3^- with $S_2O_3^{2-}$ (eqs 14 and 15) by the PAF method. Equation 13 can be treated as a preequilibrium because $k_1[I^-]$ ($= 5.6 \times 10^9$ M⁻¹ s⁻¹ \times $[0.008$ – 0.060 M]) and k_{-1} ($= 7.5 \times 10^6$ s⁻¹) are both much larger than the observed pseudo-first-order rate constants for the reactions of I_2 and I_3^- with $S_2O_3^{2-}$. The initial concentration ratios of $[S_2O_3^{2-}]/[I_2]_T$ vary from 9 to 36, so there is no possibility of I_3^- re-formation. A large absorbance decrease occurs as I_3^- disappears and the products ($I_2S_2O_3^{2-}$ and $IS_2O_3^-$) form. The A_∞ value in eq 11 refers to the equilibrium absorbance prior to the slower rate of $S_4O_6^{2-}$ formation. (The reaction in eq 17 is slow on the PAF time scale.) The A_∞ values were calculated for each set of conditions from the K_1 , K_2 , K_3 , and K_4 equilibrium constants that were evaluated from stopped-flow experiments. The A_∞ values are so small relative to A_0 that any contribution of I_3^- loss from $k_5[IS_2O_3^-][S_2O_3^{2-}]$ would have no effect on the experimental k_r values. We could not evaluate the k_4 rate constant (for the conversion of $I_2S_2O_3^{2-}$ to $IS_2O_3^-$) from our stopped-flow data, but these data indicate that $k_4 > 250$ s⁻¹. Because the value of k_4 is not known, we calculated another set of values (A_∞') based on the assumption that $I_2S_2O_3^{2-}$ is the reaction product on the PAF time scale with slower formation of $IS_2O_3^-$. These A_∞' values are also very small compared to A_0 , and there is almost no effect on the calculated k_r values. Slow formation of $IS_2O_3^-$ is not consistent with the stopped-flow data, so we report k_r rate constants based on A_∞ (i.e. rapid equilibration of $I_2S_2O_3^{2-}$ and $IS_2O_3^-$).

Table IV. Pulsed-Accelerated-Flow Data^a for I₂ and I₃⁻ Reactions with S₂O₃²⁻

10 ⁶ [I ₂] _T , M	10 ⁵ [S ₂ O ₃ ²⁻], M	[I ⁻], M	10 ⁻⁴ k _r , s ⁻¹
3.39	3.80	8.0	6.1 (3)
3.39	5.00	8.0	7.6 (9)
3.39	6.30	8.0	10 (1)
3.39	7.50	8.0	12 (1)
3.51	3.80	15.0	5.08 (9)
3.51	5.00	15.0	7.1 (3)
3.51	6.30	15.0	9 (1)
3.51	7.50	15.0	10 (1)
3.51	10.0	15.0	12 (1)
3.51	12.5	15.0	15 (2)
4.17	3.83	25.0	2.29 (2)
4.17	4.34	25.0	2.76 (4)
4.17	5.11	25.0	3.52 (9)
4.17	5.62	25.0	3.82 (5)
4.17	6.38	25.0	4.6 (1)
4.17	7.66	25.0	5.57 (9)
4.17	8.93	25.0	6.8 (1)
4.17	10.2	25.0	7.9 (2)
5.25	5.01	40.0	4.35 (8)
5.25	7.65	40.0	6.7 (2)
5.25	10.2	40.0	8.3 (6)
5.25	12.8	40.0	10.3 (3)
5.25	15.3	40.0	11.3 (5)
3.36	3.79	50.0	3.43 (1)
3.36	6.35	50.0	5.9 (7)
3.36	8.85	50.0	7.0 (3)
3.36	10.1	50.0	7.6 (4)
3.36	11.4	50.0	8.1 (4)
3.36	12.7	50.0	9.0 (3)
5.41	5.01	60.0	4.30 (9)
5.41	7.65	60.0	6.5 (2)
5.41	10.2	60.0	8.2 (2)
5.41	12.8	60.0	9.4 (4)
5.41	15.3	60.0	10.3 (3)
5.41	17.8	60.0	11.9 (4)
5.41	20.4	60.0	12.6 (6)

^a Conditions: $\mu = 0.10$ M (NaClO₄); 25.0 ± 0.2 °C; $\lambda = 353$ nm; PAF IV. PAF data were analyzed by using A_{∞} calculated from $K_1 = 721$ M⁻¹, $K_2 = 3.2 \times 10^7$ M⁻¹, $K_3 = 4.4 \times 10^4$, and $K_4 = 0.245$ M.

The rate expression from the proposed mechanism is given in eq 40 in terms of [I₂]_T (= [I₂] + [I₃⁻]) and [I₂S₂O₃²⁻]_T (= [I₂S₂O₃²⁻] + [IS₂O₃⁻]). Since the I⁻ and S₂O₃²⁻ concentrations are in excess,

$$-\frac{d[I_2]_T}{dt} = \left(\frac{k_2 + k_3 K_1 [I^-]}{1 + K_1 [I^-]} \right) [S_2O_3^{2-}] [I_2]_T - \left(\frac{k_{-2} [I^-] + k_{-3} [I^-]^2}{K_4 + [I^-]} \right) [I_2S_2O_3^{2-}]_T \quad (40)$$

this is a reversible first-order reaction between total iodine and total I₂S₂O₃²⁻. Therefore, the pseudo-first-order rate constant is given by eq 41.

$$k_r = \left(\frac{k_2 + k_3 K_1 [I^-]}{1 + K_1 [I^-]} \right) [S_2O_3^{2-}] + \left(\frac{k_{-2} [I^-] + k_{-3} [I^-]^2}{K_4 + [I^-]} \right) \quad (41)$$

Table IV gives the conditions and calculated k_r values from PAF experiments as a function of S₂O₃²⁻ and I⁻ concentrations. Figure 4 shows an experimental plot of eq 11 for decelerated flow, where $k_r = 1/(-\text{slope})b = 22\,600 \pm 200$ s⁻¹. Figure 5 shows plots of k_r against [S₂O₃²⁻] for two sets of [I⁻] concentrations (0.008 and 0.050 M). The precision for the intercept values from eq 41 is poor, because the reaction has very little reversibility. However, the precision for the slopes is satisfactory, and the forward rate constants are given by eq 42. Figure 6 shows the fit of k_r against [I⁻], where $k_2 = (7.8 \pm 0.1) \times 10^9$ M⁻¹ s⁻¹ and $k_3 = (4.2 \pm 0.1) \times 10^8$ M⁻¹ s⁻¹.

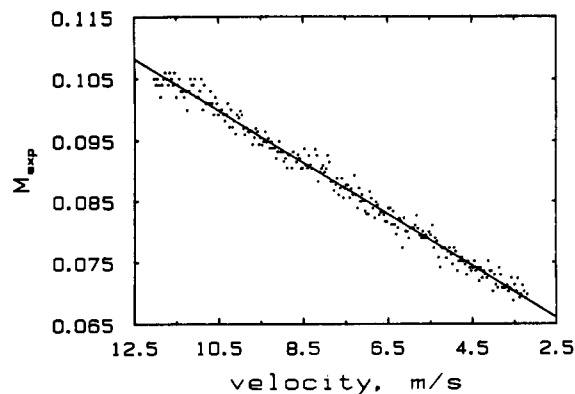


Figure 4. Experimental data for the parallel reactions of I₂ and I₃⁻ with S₂O₃²⁻ obtained by the pulsed-accelerated-flow method. M_{exp} is defined in eq 11, with $k_r = -1/b(\text{slope}) = (2.26 \pm 0.02) \times 10^4$ s⁻¹. The solid line is the least-squares fit.

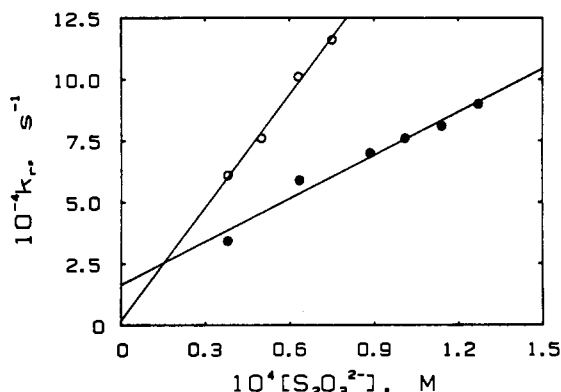


Figure 5. Thiosulfate dependence of the pseudo-first-order rate constants (k_r) for the reactions of I₂ and I₃⁻ with thiosulfate. The slope gives k_r (eq 42): (O) [I⁻] = 8 mM; (●) [I⁻] = 50 mM.

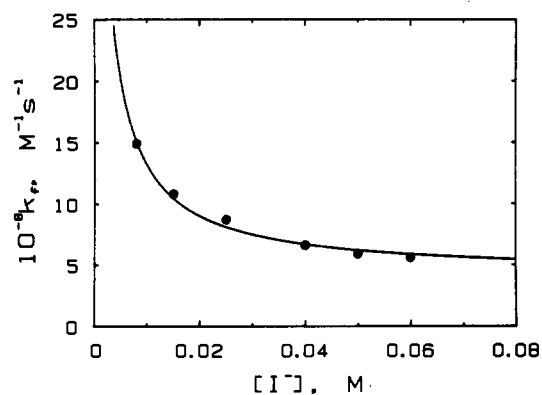


Figure 6. Iodide dependence of the forward rate constants (k_2 and k_3) for the reactions of I₂ and I₃⁻ with S₂O₃²⁻. The curve is evaluated from eq 42, where $k_2 = (7.8 \pm 0.2) \times 10^9$ M⁻¹ s⁻¹ and $k_3 = (4.2 \pm 0.1) \times 10^8$ M⁻¹ s⁻¹.

$$\text{slope} = k_r = \frac{k_2 + k_3 K_1 [I^-]}{1 + K_1 [I^-]} \quad (42)$$

A value of 7×10^9 M⁻¹ s⁻¹ is estimated²¹ for the diffusion-controlled rate constant in water at 25 °C for reactants of equal radii with no charge attraction or repulsion. Therefore, the k_2 rate constant of 7.8×10^9 M⁻¹ s⁻¹ can be considered to be a diffusion-limited value. Electrostatic repulsion would be expected to give a smaller rate constant for the reaction of I₃⁻ and S₂O₃²⁻. However, k_3 is 19 times smaller than k_2 , which is more than an

(21) Caldin, E. F. *Fast Reactions in Solution*, Wiley: London, 1964; pp 10–12.

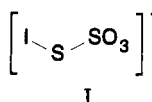
Table V. Summary of Rate and Equilibrium Constants^a

reaction	constant
$I_2 + S_2O_3^{2-} \rightleftharpoons I_2S_2O_3^{2-}$	$k_2 = 7.8 \times 10^9 \text{ M}^{-1} \text{ s}^{-1}$ $k_{-2} = 250 \text{ s}^{-1}$ $K_2 = 3.2 \times 10^7 \text{ M}^{-1}$
$I_3^- + S_2O_3^{2-} \rightleftharpoons I_2S_2O_3^{2-} + I^-$	$k_3 = 4.2 \times 10^8 \text{ M}^{-1} \text{ s}^{-1}$ $k_{-3} = 9.5 \times 10^3 \text{ M}^{-1} \text{ s}^{-1}$ $K_3 = 4.4 \times 10^4$
$I_2S_2O_3^{2-} \rightleftharpoons IS_2O_3^- + I^-$	$K_4 = 0.245$
$IS_2O_3^- + S_2O_3^{2-} \rightarrow S_4O_6^{2-} + I^-$	$k_5 = 1.29 \times 10^6 \text{ M}^{-1} \text{ s}^{-1}$
$I_2 + I^- \rightleftharpoons I_3^-$	$k_1 = 5.6 \times 10^9 \text{ M}^{-1} \text{ s}^{-1}$ $k_{-1} = 7.5 \times 10^6 \text{ s}^{-1}$ $K_1 = 721$

^a 25.0 °C; $\mu = 0.10 \text{ M}$. ^b Reference 17; 25 °C; $\mu = 0.001\text{--}0.006 \text{ M}$. ^c Reference 18.

electrostatic effect for ions of this size; consequently, the k_3 rate constant is not diffusion-limited.

$I_2S_2O_3^{2-}$ and $IS_2O_3^-$. Previous papers^{5,7,8,9} have written the formula of monoiodine thiosulfate as $S_2O_3I^-$, which implies that O–I bonds are formed. Awrey and Connick argue in favor of structure I, and we strongly concur that iodine is bound to sulfur,



not to oxygen. To emphasize this, we prefer to write the formula as $IS_2O_3^-$. The structure for $I_2S_2O_3^{2-}$ is expected to have a linear arrangement of two iodines and a sulfur, with 10 valence electrons (three nonbonding pairs and two bonding pairs) around the central iodine (structure II). Similar I_2X adducts are formed where X is chloride, bromide, pyridine, thiocyanate, or amines.

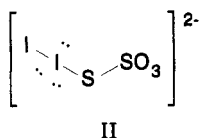


Table V summarizes the rate constants and equilibrium constants for the proposed mechanism. We conclude that $I_2(\text{aq})$ and $S_2O_3^{2-}$ form an adduct ($I_2S_2O_3^{2-}$) at diffusion-controlled rates and that the parallel reaction with I_3^- and $S_2O_3^{2-}$ is also extremely rapid. The stability constant (K_2) for $I_2S_2O_3^{2-}$ is unusually large for nucleophilic adducts with I_2 . For example, the corresponding stability constants (K_f, M^{-1}) for I_3^- , $C_5H_5NI_2$,²² and $(C_2H_5)_3NI_2$ ²² are 721, 270, and 5130, respectively. On the other hand, $S_2O_3^{2-}$ is a very strong nucleophile ($n = 6.36$ on the Swain–Scott scale compared to $n = 5.04$ for I^-).^{23,24} Table VI summarizes K_f values as a function of nucleophilicity.

The dissociation equilibrium constant (K_d, M) for $I_2S_2O_3^{2-}$ (eq 43) is relatively large compared to corresponding K_d values for I_2Cl^- and other I_2X^- species as shown in Table VI. Figure 7

$$K_d = K_4 = \frac{[IS_2O_3^-][I^-]}{[I_2S_2O_3^{2-}]} = 0.245 \text{ M} \quad (43)$$

shows an excellent correlation between the nucleophilicity of X and the ease of dissociation of I^- from I_2X^- to form IX. The stronger the X nucleophile, the larger the K_d value. Thus, the value for K_4 is quite reasonable. Figure 7 also shows the correlation of K_f values with nucleophilicity. There is much more scatter for

Table VI. I_2X Formation and Dissociation Equilibrium Constants^a

X	K_f, M^{-1}	K_d, M	n^b	ref
Cl^-	1.6	1.3×10^{-9}	3.04	c
Br^-	12.7	5×10^{-7}	3.89	d
SCN^-	85		4.77	e
I^-	721	1.39×10^{-3}	5.04	f
$S_2O_3^{2-}$	3.5×10^7	0.245	6.36	g

^a $K_f = [I_2X]/[I_2][X]$; $K_d = [IX][I^-]/[I_2X]$; 25 °C. ^b Nucleophilicity (n) values from: Hine, J. *Physical Organic Chemistry*; McGraw-Hill: New York, 1962; p 161. ^c Margerum, D. W.; Dickson, P. N.; Nagy, J. C.; Kumar, K.; Bowers, C. P.; Fogelman, K. D. *Inorg. Chem.* **1986**, *25*, 4900–4904. ^d Troy, R. C.; Kelley, M. D.; Nagy, J. C.; Margerum, D. W. *Inorg. Chem.* **1991**, *30*, 4838–4845. ^e Lewis, C.; Skoog, D. A. *J. Am. Chem. Soc.* **1962**, *84*, 1101–1106. ^f Reference 18. ^g This work.

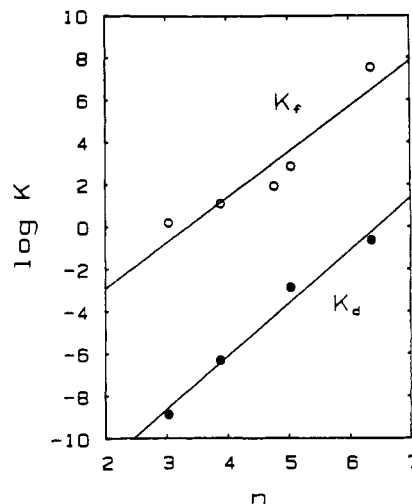
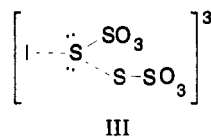


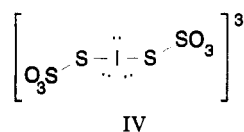
Figure 7. Dependence of the I_2X ($X = Cl^-, Br^-, SCN^-, I^-$, or $S_2O_3^{2-}$) stability constant ($K_f = [I_2][X]/[I_2X]$) and dissociation constant ($K_d = [I^-][IX]/[I_2X]$) on the nucleophilicity (n) of the anions.

K_f than for the K_d correlation, but the trend indicates that a large value of K_f should be expected with $S_2O_3^{2-}$. The soft-acid and soft-base character of the reactants should also help to give a stable adduct.²⁵ The relatively large values for the slopes in Figure 7 (2.6 for $\Delta(\log K_d)/\Delta n$ and 2.1 for $\Delta(\log K_f)/\Delta n$) indicate that both sets of equilibrium constants are very sensitive to the nucleophilicity of the adduct.

$S_2O_3^{2-}$ Attack on $IS_2O_3^{2-}$. The proposed transition state (structure III) has $S_2O_3^{2-}$ attack at the sulfur atom of $IS_2O_3^-$ with I^- elimination to give $S_4O_6^{2-}$. The possible formation of an



intermediate was considered where $S_2O_3^{2-}$ reacts at the iodine atom of $IS_2O_3^-$ to give $I(S_2O_3)_2^{3-}$ (Structure IV). This species



was considered for conditions where the initial $S_2O_3^{2-}$ concentration was greater than twice the initial total iodine concentration. If $I(S_2O_3)_2^{3-}$ formed, it would have no effect on the PAF data for the determination of k_2 and k_3 . However, an appreciable

(22) Drago, R. S. *Physical Methods in Chemistry*, Saunders, Philadelphia, PA, 197; p 121.

(23) Swain, C. G.; Scott, C. B. *J. Am. Chem. Soc.* **1953**, *75*, 141–147.

(24) Hine, J. *Physical Organic Chemistry*; McGraw-Hill: New York, 1962; p 161.

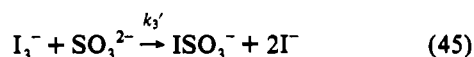
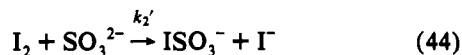
(25) Pearson, R. G. *Proc. Natl. Acad. Sci. U.S.A.* **1986**, *83*, 8440–8441.

(26) Klopman, G. *J. Am. Chem. Soc.* **1968**, *90*, 223–234.

(27) Ho, T. L. *Hard and Soft Acids and Bases in Organic Chemistry*, Academic: New York, 1977.

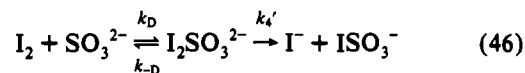
concentration of $I(S_2O_3)_2^{3-}$ would affect the stopped-flow data used to evaluate k_5 . The result would be a saturation effect as the $S_2O_3^{2-}$ concentration increased, because $I(S_2O_3)_2^{3-}$ would be expected to be a very labile side product. Figure 1 shows no evidence of a saturation effect with $S_2O_3^{2-}$ concentration, and therefore the equilibrium constant for $[I(S_2O_3)_2^{3-}]/([IS_2O_3^-][S_2O_3^{2-}])$ must be less than $500 M^{-1}$. On the other hand, we would expect this equilibrium constant to be greater than $1/K_4 = 4.08 M^{-1}$, because $S_2O_3^{2-}$ is a stronger nucleophile than I^- . Under our conditions the $S_2O_3^{2-}$ concentration was too low to form appreciable amounts of $I(S_2O_3)_2^{3-}$.

Comparison of SO_3^{2-} and $S_2O_3^{2-}$ Reactions with Iodine. PAF methods were used previously²⁸ to measure rate constants for SO_3^{2-} reactions with I_2 and I_3^- (eqs 44 and 45), where $k_2' = 3.1$



$\times 10^9 M^{-1} s^{-1}$ and $k_3' = 2.9 \times 10^8 M^{-1} s^{-1}$ at $25.0 \pm 0.2^\circ C$ and $\mu = 0.50 M$ ($NaClO_4$). The corresponding $S_2O_3^{2-}$ reactions are faster with $k_2/k_2' = 2.5$ and $k_3/k_3' = 1.5$. An intermediate species, $I_2SO_3^{2-}$, was suggested.²⁸ However, the observed kinetics did not require that it be an intermediate rather than a transition state. Since $I_2S_2O_3^{2-}$ is required from the thiosulfate kinetics, it is of interest to compare these two iodine adducts. Our correlation of K_f values with nucleophilicity suggests that $K_f' = [I_2SO_3^{2-}]/([I_2][SO_3^{2-}])$ will be approximately $720 M^{-1}$, because the nucleophilicity of SO_3^{2-} is the same as I^- and this is the value for K_1 . Under the conditions used by Yiin and Margerum,²⁸ the maximum SO_3^{2-} concentration was $0.64 \times 10^{-4} M$. Hence, the

maximum ratio of $[I_2SO_3^{2-}]/[I_2]$ would be 0.046, which is too small to be observed. If we treat $I_2SO_3^{2-}$ as an intermediate, we would expect this adduct to form with a diffusion-controlled rate constant (k_D) in accord with eq 46. A steady-state treatment



gives eqs 47 and 48. This suggests that the breakup of $I_2SO_3^{2-}$

$$k_2' = \frac{k_D k_4'}{k_{-D} + k_4'} = k_D \left(\frac{1}{\left(\frac{k_{-D}}{k_4'}\right) + 1} \right) \quad (47)$$

$$\frac{k_{-D}}{k_4'} = \frac{k_D}{k_2'} - 1 = \frac{7.8}{3.1} - 1 = 1.5 \quad (48)$$

to form I^- and ISO_3^- contributes to the less-than-diffusion-controlled value observed for the reaction between I_2 and SO_3^{2-} . The estimated stability constant $K_f' = k_D/k_{-D} = 720 M^{-1}$, so k_{-D} is estimated to be $1.1 \times 10^7 s^{-1}$. This is similar to the k_{-1} value of $0.85 \times 10^7 s^{-1}$ for I_3^- . This suggests that $k_4' = 1.1 \times 10^7/1.5 = 7.2 \times 10^6 s^{-1}$.

Conclusions

Aqueous iodine reacts at diffusion-controlled rates with thiosulfate to give an $I_2S_2O_3^{2-}$ adduct. This adduct rapidly dissociates to give I^- and $IS_2O_3^-$, and the latter species reacts with additional $S_2O_3^{2-}$ to give $S_4O_6^{2-}$ and I^- . The rate constants are summarized in Table V. The corresponding reaction of $I_2(aq)$ with SO_3^{2-} is 2.5 times slower. This is attributed to a contribution from the breakup of the $I_2SO_3^{2-}$ adduct to form I^- and ISO_3^- .

Acknowledgment. This work was supported by National Science Foundation Grants CHE-8720318 and CHE-9024291.

(28) Yiin, B. S.; Margerum, D. W. *Inorg. Chem.* 1990, 29, 1559-1564.